Supplementary Materials

1. ADMA focussing array

The ADMA concept enables the engineering of the shape of an ion cloud beam, aiming to increase the performance of an ion-separating device. In this paper, the ion cloud formed in the ionisation chamber was focused in one dimension using an electric field to counteract diffusion broadening. An experimental apparatus was constructed (Fig. 1). This comprises an ion source (^{63}Ni in the form of a cylindrical foil), a rectangular flow channel containing the electrodes, and an ion detector (an Analogue Devices CN0407 data acquisition board and custom PCB). On both sides of one axis of the rectangular channel, there are six electrodes with variable voltages, while the other axis has a single fixed voltage on both sides. The apparatus allows for moving the beam of ions relative to the detector via a moveable table controlled by a micrometre screw. It also allows for the rectangular electrode channel to be rotated at 90°. Thus, precise measurements can be made of the beam profile on two axes. In addition, a removable metal shim with a rectangular slit (0.3x2.5 mm) was positioned after the electrode array. A separate voltage could be applied to this top shim. Experiments were performed with and without a second shim, which was located next to the PCB detector and is referred to here as the outlet shim.

Prior modelling showed that a particular set of voltage profiles for the multi-electrode axis should provide an optimal ion cloud shape. These voltages were optimised empirically and are shown in Table 1.

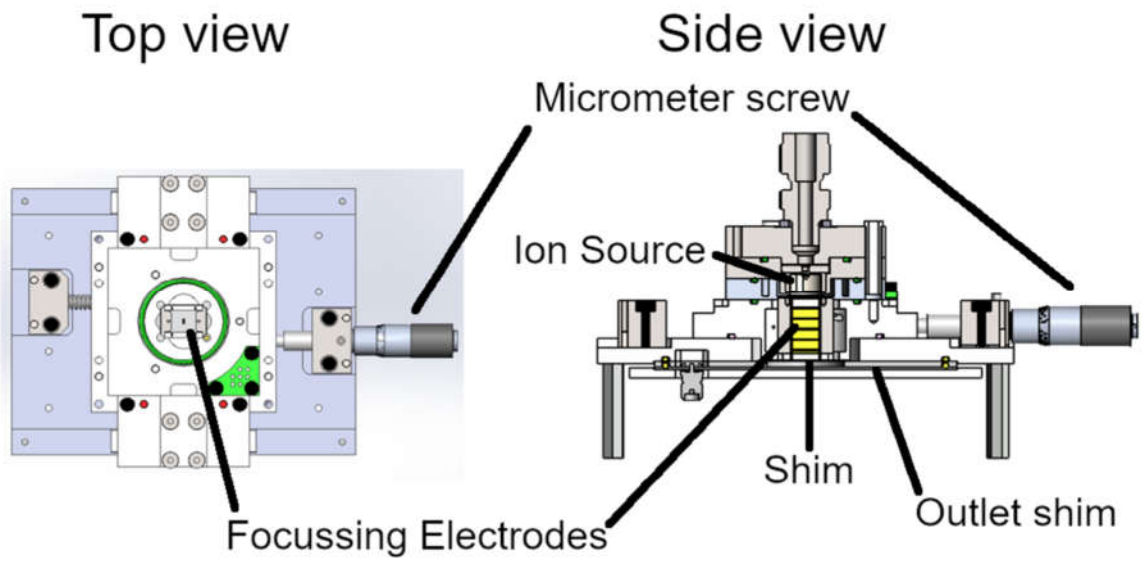

Figure 1. Schematic of the focussing electrode apparatus.

A schematic of the wiring is shown in Fig. 2. This includes the position of the outlet shim, as discussed further on in this supplement. Using these settings and the first shim, the

FWHM of the ion cloud profile along the focussing axis was initially found to be around 90 μm. Without the shim, the FWHM was measured at ~350 μm. This indicates that the slot of the shim has a prominent role in shaping the ion cloud as it was initially observed in the numerical modelling of the apparatus.

Table 1: Electrode voltages on the ion source and focussing array.

Electrode position	**Voltage (V)**
Ion Source	1000
1	997.8
2	991.8
3	963.5
4	870.0
5	639.9
6	290.0

The shape of the cloud was recovered using data from two axes and is shown as an example in Fig. 3. Several parameters in the setup affected the shape, such as the base voltages (i.e., the proportional increasing or decreasing of the ion source and electrode voltages). Other parameters include the flow rate through the ion source, the ion source offset voltage, the voltage on the shim, and a steering offset voltage on the electrodes (i.e., greater on one side to allow steering of the cloud). Lower base voltages lead to thinner values for the cloud thickness, but at the cost of lower ion current. Higher values for the shim voltage gave thinner values for the cloud with no cost to the ion current. However, in a practical system, the shim voltage is analogous to the scanning voltage of a system, where each value for the voltage corresponds to ions with certain electrical mobility.

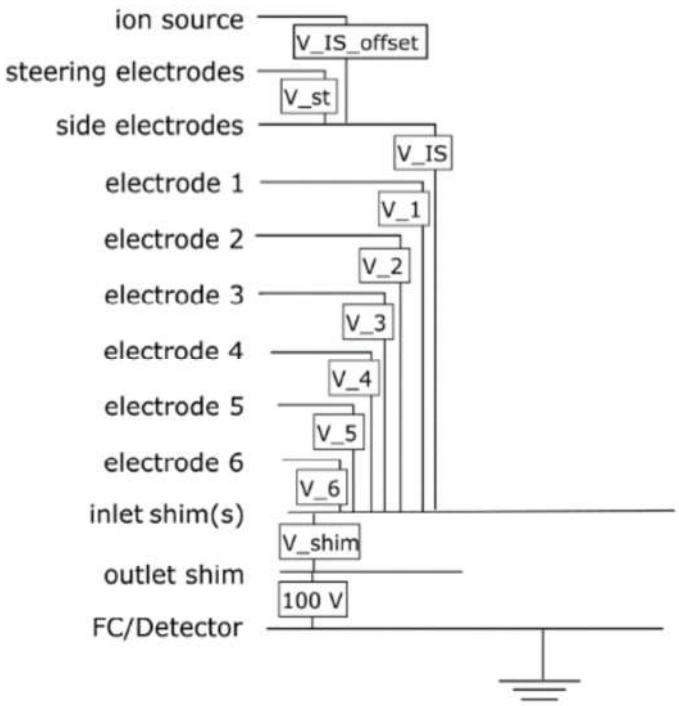

Figure 2. Schematic of the wiring for the focussing array setup (voltages are shown in Table 1).

Experimental data were gathered on over 100 different configurations of the parameters affecting the thickness of the ion cloud and used to train a machine learning (ML) algorithm. This was used to predict the ion cloud shape values for different parameters without empirical data for those settings. The best predicted settings were then used empirically to get more data for the ML algorithm to train on. This procedure allowed optimisation of the ion beam to best values of around FWHM = 30 μm for the ion cloud thickness (with an ion current at the detector of about 20 pA).

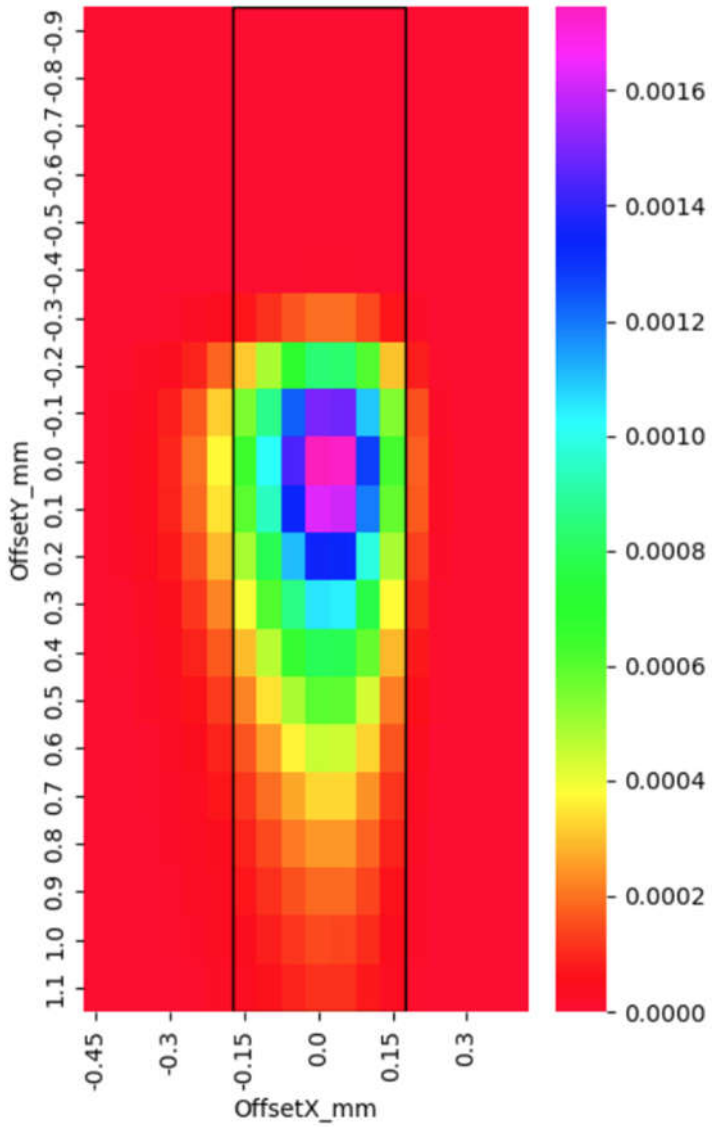

Figure 3. Ion beam profile at the detector electrode. The colour scale shows the ion current per unit area.

Data were also obtained by varying the base voltage profile on the focusing array. Many variations of ion source focussing array voltage were tested (a combination of similar voltages to those shown in Table 1 and random values in the ranges 100 -1200 V). A new ML algorithm was trained using the empirical data obtained for each voltage profile, and predictions were made for optimum values of the thickness of the ion cloud. This did not lead

to any useful improvement in the values, which confirms that the initial values for the electrode voltages were already successfully optimised by numerical modelling.

Tests were carried out to assess the impact of the thickness of the shim. A double - thickness shim was formed by fixing two shims together using silver conductive paint. The thickness of the ion cloud was unaffected by this change (FWHM ~ 40 μm). However, the dependency of the ion cloud thickness on the value of the base voltage seemed to be removed in the range of base voltages from 300 to 1200.

Further experiments were performed with an additional shim on the outlet. These shims were fixed and positioned such that the slots were directly over the detector electrode. Three different outlet shims were tested, with slot widths of 0.10, 0.15, and 0.20 mm (all with 3.0 mm length slits). It was possible to reduce the ion cloud thickness (slot width = 0.15 mm) to around 27 μm (± 3 μm), but at the cost of much lower ion current at the detector (~ 3 pA). At a slot width of 0.10 mm, the ion current was ~ 30% lower still.

2. Comparison of the ADMA and DMA with electronic nose methods

The main challenges that electronic nose works face are: the non-specificity of the individual nanosensors; a low information density that is required for a TVD detection vapour at low concentrations of trace compounds (ppt-ppq); and an insufficient repeatability of the detection in challenging environments, e.g., caused by variations of the humidity and concentrations of other atmospheric constituents. These challenges may impact the transition time from a laboratory device to field applications.

Moreover, the super-sensitive method reported by Engel *et al*. (2010) reveals that the number of individual nanosensors N_{is} may be relevant to the absolute low detection limit of the method. Indeed, to achieve good reproducibility in the pattern of the detector response to a challenge analyte, two conditions need to be met:
1) the $N_{is} >> 1$, and
2) the number of challenge molecules in a sample ($N_c >> N_{is}$), where the number of challenge molecules in a sample is N_c.

The first condition is derived from the complexity of the air chemical composition at very low mixing ratios (ppt and ppq); see, for example, Amman and Smith (2013). There are circa 10^4 different gaseous chemicals at STP conditions in the air. Furthermore, these atmospheric compounds are unstable and exhibit well-documented temporal and spatial variations in atmospheric chemistry. To identify trace amounts of analytes in the air, the information density of the method should be close to or greater than the same as for GS-MS or GC-IMS 2D spectra. It is rather difficult to evaluate the number of individual nanosensors (N_{is}) in a device to satisfy this condition, but it most likely should be around 10^4 to be close to the GC-MS method.

The second condition is a statistical requirement for uniformity in the distribution of analyte molecules in the plurality of individual nanosensors. If $N_c < N_{is}$ or $N_c = N_{is,}$ then the

reproducibility of the sensor response might be influenced by the statistics of the analyte molecule distributions over the individual nanosensor population. This complicates the interpretation of data and may affect the reproducibility of analyte recognition.

The theoretical low-detection limit of the super-sensitive method by Engel *et al*. (2010) may require a lot of molecules to be processed by the device. On the contrary, the theoretical low-detection limit for the IIC method is only 1 ion (Gorbunov *et al*., 2018). The IIC is a direct single-ion counting method, so statistical constraints are not relevant to it. This consideration is applicable to other electronic nose methods (Burton and Gorbunov, 2018). Therefore, the ADMA-IIC method seems to be more suitable for the TVD than methods based on the electronic nose concept.

3. Influence of ion mobility on the resolving power

The RP for the spectra presented in Figs. 3–5 is influenced by the separation voltage and, therefore, by the ion mobility; see expression (2). The greater the ion mobility, the lower the RP (Fig. 4). The increase in ion mobility from 0.7 $cm^2/V/s$ to 1.5 $cm^2/V/s$ is decreasing the RP from ~ 100 to ~ 50 $cm^2/V/s$. The spread of data points around the trend line is most likely caused by the influence of the shape and mass of the analytes on the diffusivity and ion mobility. Thus, it is an advantage of the ADMA as well as the ion DMA to separate larger analyte molecules or cluster analytes from reagent ions.

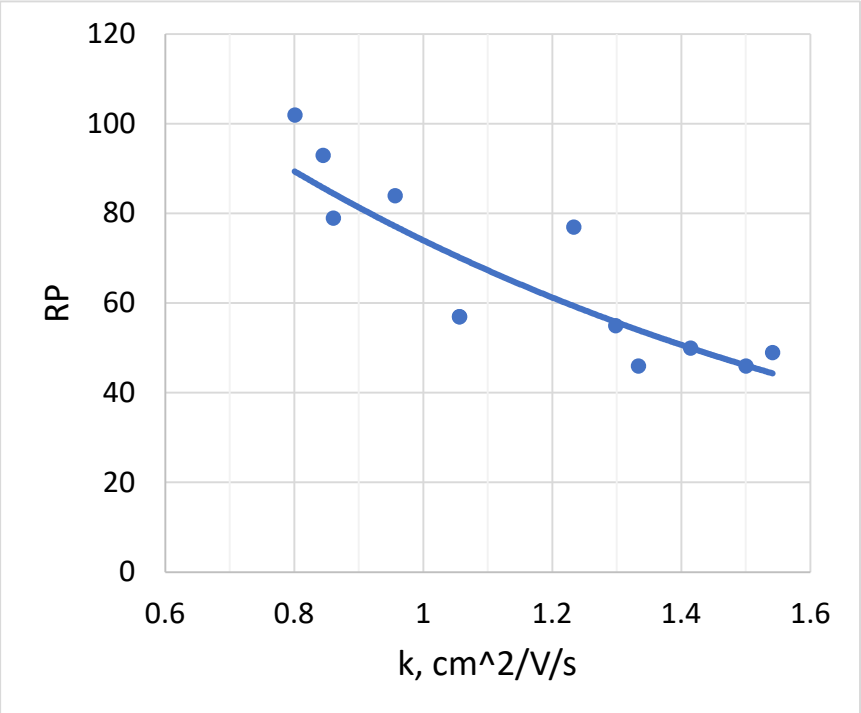

Figure 4. The RP for the spectra presented in Figs. 3–5 vs. the ion mobility. Two points where IP = 94 and 102 (top left) were not identified.

4. Concentration of analytes in the sample and the IIC detector

The mixing ratios for the explosives and organophosphorus compounds were in the low ppb to ppq ranges. It is very difficult to measure the concentration of analyte in samples at such small levels. On the contrary, the ion concentrations in the IIC detector can be found from tagged ion number counts measured by the OPC.

The intensity of the spectra, measured by the IIC, is the number of counts per second. The flow rate of selected ions was 0.3 l/min; therefore, the ion concentration (IC per cm^3) measured by the OPC was the IIC Intensity/5. For example, for the trimer of DIMP (Fig. 3 of the main text), the largest peak maximum IC is 4,800/5 = 960 cm^{-3}, or 36 ppq. The smaller trimer peak has IC = 3,000/5 = 600 cm^{-3}, or 22 ppq.

The dimer's largest peak IC is 4,750/5 = 950 cm^{-3}, or 35 ppq. It is very close to the largest trimer peak. However, the smallest dimer peak has an IC of 100/5 = 20 cm^{-3}, or 0.7 ppq or 700 parts per quintillion (700 ppql).

The monomer's largest peak IC is 1,510/5 = 302 cm^{-3}, or 11 ppq. The smallest monomer peak has an IC of 50/5 = 10 cm^{-3} or 0.35 ppq, or 350 parts per quintillion (350 ppql).

The ion number concentration in the IIC detector is linked to the analyte concentration in the sample inlet; $IC = C_{analyte} \cdot \gamma$, where γ is the correction coefficient influenced by the ionisation efficiency, ion tagging efficiency and other factors. These efficiencies and factors are determined by the design of the IIC and ADMA. The theoretical limit of the correction coefficient is 100%. For the current version of the ADMA-IIC, the γ estimates are from 0.1 down to 10^{-2}. The evaluation of the correction coefficient was not the subject of this publication. Importantly, with a realistic correction factor of 10^{-2}, the analyte concentration that could be detected in the current version of the ADMA-IIC design is in the ppq range.